Estimating snapping shrimp noise in warm shallow water

Hong LI[1], Teong Beng KOAY[1], John POTTER[2] & Sim Heng ONG[3]

[1]Research Engineer, Department of Electrical Engineering,
National University of Singapore

[2]Associate Professor, Acoustic Research Laboratory,
EE Dept. & TMSI,
National University of Singapore

[3]Senior Lecturer, Department of Electrical Engineering,
National University of Singapore

1 ABSTRACT

Snapping shrimp noise is thought to be a major component of ambient noise at high frequencies (2 kHz - 300 kHz) in warm shallow water. We have designed an experiment to investigate its temporal and spatial distribution and variability. This information has application to many underwater acoustic systems in providing background knowledge about the structure of this class of noise. The experiment requires a stochastic tomographic inversion to estimate the source structure from data collected by several directional hydrophones. Existing tomographic techniques have been extended to benefit from the broadband nature of the data. The experiment has been modelled by including the receiver directionality, possible source distributions and several sources of noise in the signal processing. Source distribution models have been developed and calibrated for consistency with actual shallow-water acoustic records. We develop three noise models; system noise, observational noise and beampattern uncertainty. The simulation results indicate that our stochastic inversion algorithm is robust to reasonable levels of these types of noise. We anticipate that the experiment will be able to image shrimp noise intensity on the seabed over an area of some 350 m^2 with a resolution of 3.5 m^2 and with an rms error below 20%, or approximately 0.8 dB.

2 INTRODUCTION

As part of the development of ocean technology, ambient noise has been investigated for many years. On one hand this noise leads to many limitations on underwater sonar applications, and on the other it can be used constructively in some techniques such as ambient noise imaging [1]. Our research lays particular emphasis on snapping shrimp noise, which is thought to be the main component of ambient noise in warm shallow water at high frequencies [2]. Based on tomographic technology, we have designed an underwater acoustic experiment to learn more about these animals, specifically the temporal and spatial characteristics of their sound. A preliminary description of the inverse method was presented in an invited paper at the Shallow Water Acoustics Conference in Beijing in 1997 [3]. In this paper we extend the

sophistication of the algorithm to include three system and observation noise models and to give some results of testing the robustness of the inversion to these perturbations. In addition, we estimate the number of shrimp snaps per square metre per second in a local area near Singapore.

The technologies of computerised tomography (CT), and ocean acoustic tomography (OAT) are well developed. These traditional tomographic techniques normally rely on placing a network of receivers and some deterministic, controlled sources around a volumetric region. The sources are used to make transmissions to certain or all receivers and the travel time or absorption of emission during the travel path is recorded. Various algorithms have been developed for different situations. The term stochastic tomography refers to the sources being stochastic, rather than deterministic. Instead of being located at the outer edge of the region of interest, they are randomly distributed within the area bounded by the receivers. The estimated field is that of the active sources themselves, not a passive medium. Accordingly, the inversion is for an areal, not a volumetric structure where these sources are confined to a layer on or very near the seabed.

Most OAT applications interpret the travel time or other acoustic parameters which are functions of temperature, salinity, water velocity, etc. This provides information about the intervening ocean, typically mesoscale variability which occurs with spatial scales of tens or hundreds of kilometers and with temporal scales of tens or hundreds of days. A recent technique that focuses on smaller scales in the ocean has been published by Pidsley and Davies who classify seabed objects by acoustic means [4]. Their technique is based on the circumnavigation of source and detection facilities around the object under examination. In their work, the procedure was simulated in the laboratory by a turntable holding the objects. However, it is not yet practical for use in the ocean.

The term “stochastic tomography” has been used in an earlier publication [5], which investigated techniques for ionospheric estimation on the scale of hundreds or thousands of kilometers. As far as we are aware the term has not been used, nor the method applied, for ocean acoustics. The target of our interest is a two dimensional random source distribution on or near the sea bed. The propagation properties of the ocean are assumed known and stationary in the short range and time involved. Since acoustic receivers instead of sound generators are required for the proposed experiment, it is a type of passive tomography. Moreover, our estimation is expected to calculate the source variability over a spatial scale of several meters, and over a temporal scale of a few hours, rather than mesoscales.

3 EXPERIMENTAL DESIGN & SIMULATION

As outlined in [3], the experiment utilizes some receivers to surround a small region of seabed, perhaps 20-40 meters in diameter, containing snapping shrimp. The receivers are six directional hydrophones, raised above the bottom and angled downward. Each directional hydrophone will have a narrow receiving beam, achieved by means of a parabolic acoustic lens. A contour of constant receiving sensitivity from such an axially-symmetric beam, incident at some angle to a plane seabed, will then be elliptical. By panning these directional hydrophones across the region of interest, many such overlapping elliptical 'footprints' can be sampled. Each of the six directional hydrophones is located at a vertex of a hexagon (Figure 1).

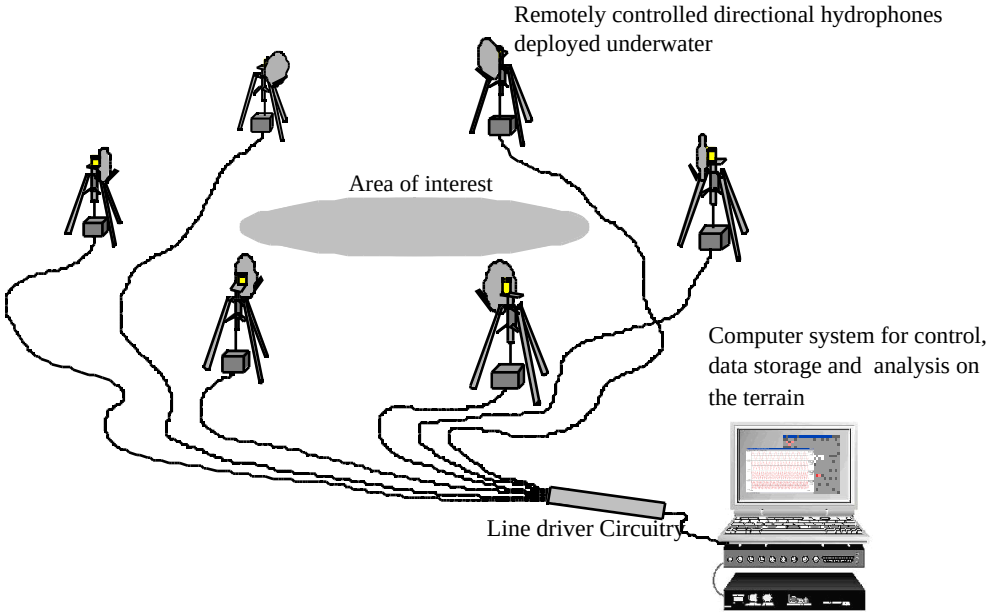

Figure 1. Schematic of the experimental arrangement on the seabed, not to scale.

In principle, it seems that we should be able to invert these data to estimate the source energy distribution in the region under examination, providing (a) we establish large enough patches on which the inversion is based, and (b) we have sufficient dimensions in the original data to ensure a stable and unique inverse. This constitutes a kind of "stochastic tomographic inversion", where the sources are the unknown and their statistically-varying parameters are what we seek to estimate.

3.1 Geometric preparation and problem establishment

The geometric diagram sketched in Figure 2 shows one such elliptical 'footprint' in heavy line, with its characteristic major and minor axes, *2a* and *2b* respectively. The lower panel of Figure 2 shows the elevation view, with the height of the directional hydrophones, *h*, characteristic half-beam width, α, beam dip angle, β and the distance between two opposite hydrophones, *d*.

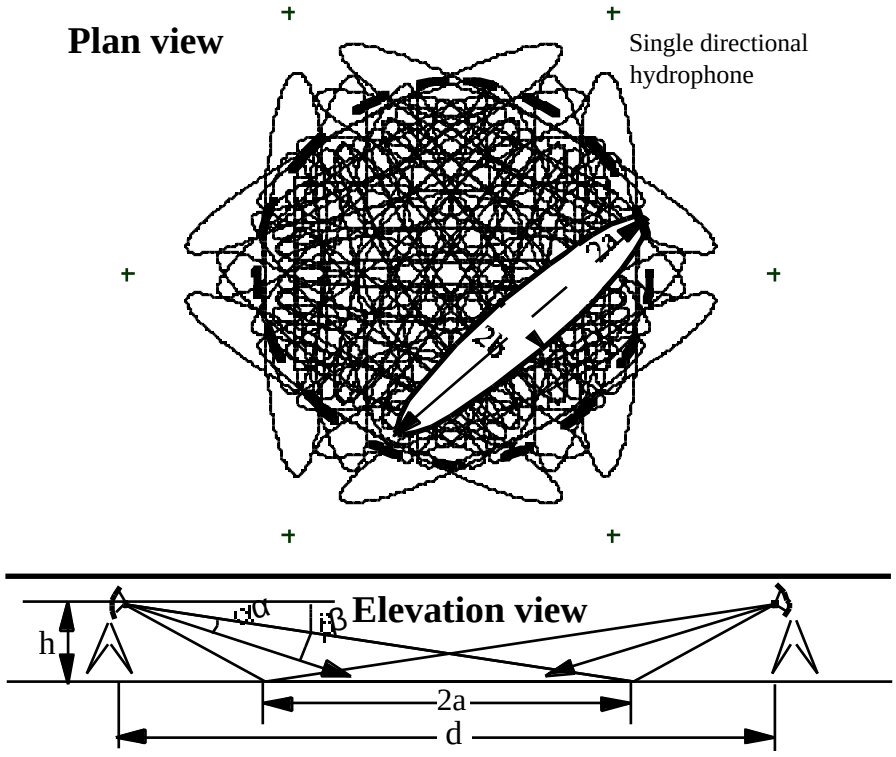

Figure 2. Geometric diagram

Geometric preparation includes computations based on some original parameters, including α, β and h. Firstly, a, b and d can be obtained by direct geometric derivation. Secondly, the approximate ranges for patch size and inversion number can be obtained. The patch size represents the physical resolution of the inversion. The sound energy distribution is represented by the average sound intensities of a number of square patches covering the target area. The inversion number is the number of patch intensities that can be estimated, which can be no greater than the number of independent pieces of information we may collect.

As described in [3], if the whole target area is split into M patches and K observations is taken for inversion, a linear algebra statement is established,

$$\mathbf{C}\bar{\mathbf{I}} = \mathbf{E}. \tag{1}$$

where $\mathbf{E}$ is an observation vector with K elements, $\mathbf{C}$ is a coefficient matrix, which can be calculated a-priori, and $\bar{\mathbf{I}}$ is the intensity field that we are estimating.

In general, we can expect the coefficient matrix to be ill-conditioned, since the receiver footprints overlap. A non-negative least squares algorithm (NNLS) [6] is adopted to provide a solution for the given problem. The standard normalised error (SNE) is taken to evaluate the performance of an inversion. The SNE level of a certain inversion is given by,

$$SNE = \frac{\sum_{i=1}^{M-1} (\hat{I}_i - I_i)^2}{\sqrt{\sum_{i=1}^{M-1} \hat{I}_i^{\,2}} \sqrt{\sum_{i=1}^{M-1} I_i^2}}, \qquad (2)$$

where $\hat{I}_i$ denotes the estimate of the energy level of the *i*-th patch inside inversion area, and $M-1$ is the number of inversion patches.

3.2 Using broadband signals

Our directional hydrophone consists of a parabolic reflector with a modified sensor (otherwise omni-directional) located at the focus of the reflector, supported by a tripod. The sensitivity as a function of angle has been evaluated using the Helmholtz-Kirchoff integral method given the physical configuration of the reflector. It displays the expected nulls and side lobes arising from the finite aperture with strong frequency dependence, as shown in Figure 3. This allows us to usefully combine the coefficients for several frequencies, treating them as from separate beams in effect, raising the rank of the coefficient matrix **C**. We can then estimate the intensity from a larger number of patches.

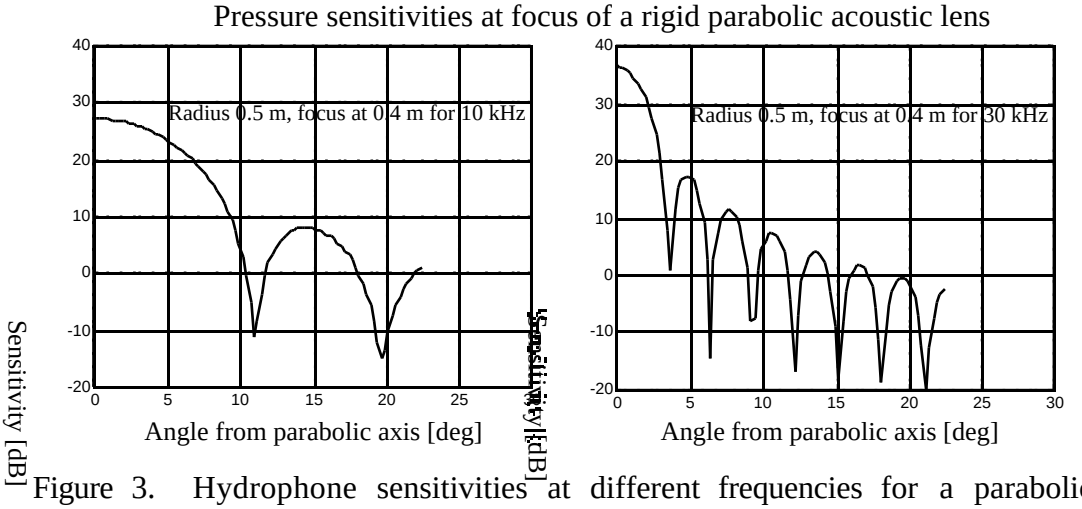

Figure 3. Hydrophone sensitivities at different frequencies for a parabolic reflector. The left panel displays results for 10 kHz, the right one for 30 kHz. The vertical axis is in dB units of intensity re the free field intensity.

Besides extending the signal to broadband, we may also choose the number of azimuthal hydrophone positions that cover the area of interest, *n*, such that *n>a/b.* This means that adjacent footprints from a directional hydrophone will overlap considerably. Although the overlapping beams result in correlation within the collected information, we can achieve a slightly greater independency in the observations. In numeric testing, we opted to use *n=4(a/b),* which is a compromise between system complexity and improved performance.

Sensitivity functions at nearby frequencies are correlated to some extent, which indicates that the rank of the coefficient matrix **C** will be significantly less than its dimension. The further apart the frequencies used in the broadband inversion, the greater the independence. We have opted to use the data at three different frequencies. Therefore, the rank, *R*, is in the range from *n*(a/b)* to *n*3*4(a/b)*. This is the constraint on the number of patches for which we may estimate intensities, the inversion number. From many simulation trials, we find that we need to choose the inversion number to be 2 to 3 times the lower bound to give the best results.

3.3 Source generator

We have developed a distribution model that we anticipate to be similar to the real environment and independent of the above parameters. We simulate the source field as an incoherent sum of snaps from sources randomly distributed according to a two-scale model. The model has an outer scale, representing the separation of groups of sources, and an inner scale, representing inter-source separation. The outer scale is intended to correspond to the distribution of suitable shelters for the shrimp to colonise, the inner scale their random colonisation of the space. The groups are randomly distributed in the area of interest with a constant probability distribution function. The shrimp locations inside a given group are normally distributed around the group center. All snaps are assumed of equal amplitude. We model an area large enough to cover all possible areas of interest in our experiment, which may be a square area up to 40 meters on a side.

The frequency of occurrence and intensity of snaps influences the simulation and the experiment dramatically. It is obvious that a few snaps with small sound intensity would be difficult to resolve. Following accessible references [7,8] and data collected by a previous experiment carried out in coastal waters near Singapore, we are able to provide an approximate estimate of the characteristics of snapping shrimp distributions, specifically the occurrence of snaps over unit area during unit time.

The estimate is obtained by comparing the spectrum intensity of a typical single snap with the recorded intensity of snapping shrimp data collected from Singapore waters. Applying an integral method that includes frequency-dependent absorption allows us to estimate, with least-squared error, the number of snaps per square metre per second. The frequency of occurrence is calculated to be 0.69 snaps per square meter per second. This estimate is consistent with other references [2,9]. The estimation provides an important parameter for the source generator of the simulation. An example of a simulated distribution is shown in Section 6.

3.4 Noise models

In a real environment, various noise sources will likely arise in the experiment and data collection. We have identified three noise sources that we believe to be the main sources of uncertainty for the experimental inversion.

Beam-pattern sensitivity noise

The non-ideal reflector and the non-ideal sensor cause beam-pattern sensitivity noise in the hydrophone system. The sensitivity function calculated by the Helmholtz-Kirchoff integral method includes diffraction but is nevertheless based on an ideal parabolic reflector and assumes that the hydrophone is placed exactly at the focus. Furthermore, the hydrophone was assumed to have a perfectly flat response with frequency.

We have modelled these composite error sources as $N_1(\theta)$, a two-component additive noise consisting of $N_{1,1}(\theta)$ due to the imperfect reflector and $N_{1,2}(\theta)$ due to random unwanted scattered noise. The directional hydrophone sensitivity is then given by

$$\bar{H}(\theta) = H(\theta) + N_1(\theta); \tag{3 a}$$

$$N_1(\theta) = N_{1,1}(\theta) + N_{1,2}(\theta) \tag{3 b}$$

where $H(\theta)$ and $\bar{H}(\theta)$ denote sensitivity functions before and after noise is added and θ is the receiving direction. $N_{1,1}(\theta)$ is assumed to be 6 dB variance Gaussian noise with mean value 20 dB lower than the envelope of the ideal beam sensitivity at different angles. $N_{1,2}(\theta)$ is taken as zero-mean and 2 dB variance white noise. The result is that $N_1(\theta)$ is dominated by the first component near the beam axis and by the second component far from the beam axis (Figure 4).

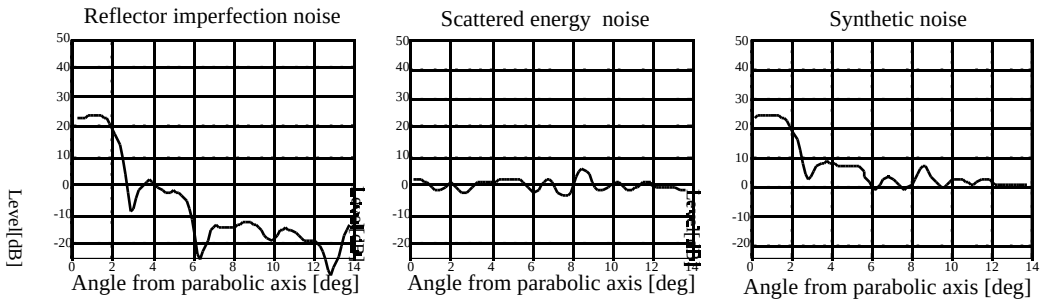

Figure 4. Beam pattern sensitivity noise and its components. (a) reflector imperfection noise, $N_{1,1}(\theta)$. (b) scattered wave noise, $N_{1,2}(\theta)$. (c) total additive beam pattern sensitivity noise, $N_1(\theta)$. The vertical axis is in dB units of intensity re the free field intensity.

An example of the impact of the total beam sensitivity noise on the beampattern of a directional receiver is illustrated in Figure 5.

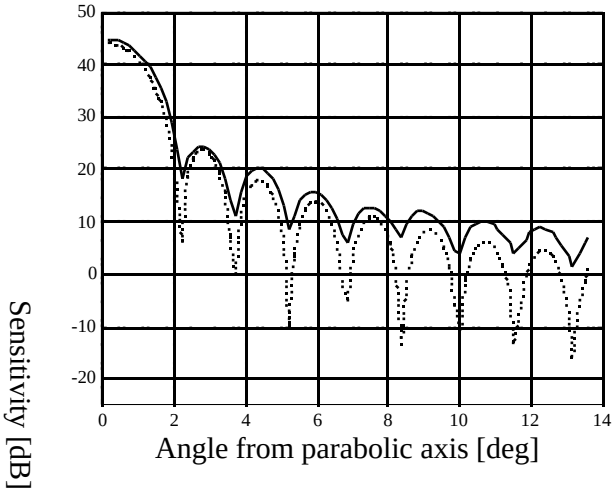

Figure 5. Sensitivity functions before and after beam sensitivity noise is added. The dashed line is a 'clean' sensitivity function obtained from Helmholtz-Kirchoff integral method. The solid curve is the disturbed sensitivity. The vertical axis is in dB units of intensity re the free field intensity.

Electronic noise

Electronic noise results from thermal noise at the input stage of the first amplifier, additive noise encountered during data transmission, filtering, amplification and digitisation. It is assumed to be zero-mean additive white noise. Various levels of noise were used in testing the inversions, from –20 to –60 dB.

Beam direction uncertainty

In the experiment, the directional hydrophones will pan in azimuth to collect data from various parts of the area of interest. Remotely controlled electric step motors with an integral direction sensor feedback drive the directional hydrophones. Despite this sophisticated directional control, imperfections in electronic and mechanical properties will result in some directional error. The sensitivity functions drawn in Figure 3 indicate that a small error in beam direction may result in significant sensitivity error because of the steep slope of the main-lobe of the sensitivity function. According to manufacturer's specifications, a typical step motor can offer an accuracy of ± 0.2 degee/step, and this has been taken as the expected heading error for an additive zero-mean Gaussian heading noise.

4 SIMULATION RESULTS

We have simulated the experimental inversion by extending the inversion algorithm described in [3] to include our three new noise mechanisms and snapping shrimp distribution model. A Monte-Carlo method was employed to obtain inversion error statistics. As the dependence of the error on the choice of geometric parameters was explored, a steepest-descent technique was used to optimise the geometric experiment parameters to obtain the best spatial resolution and robust inversion in the presence of noise. The spatial dependence of the error indicates that the inversion is more reliable inside the annular region 0.15 – 0.80 of the radius of the entire inversion region.

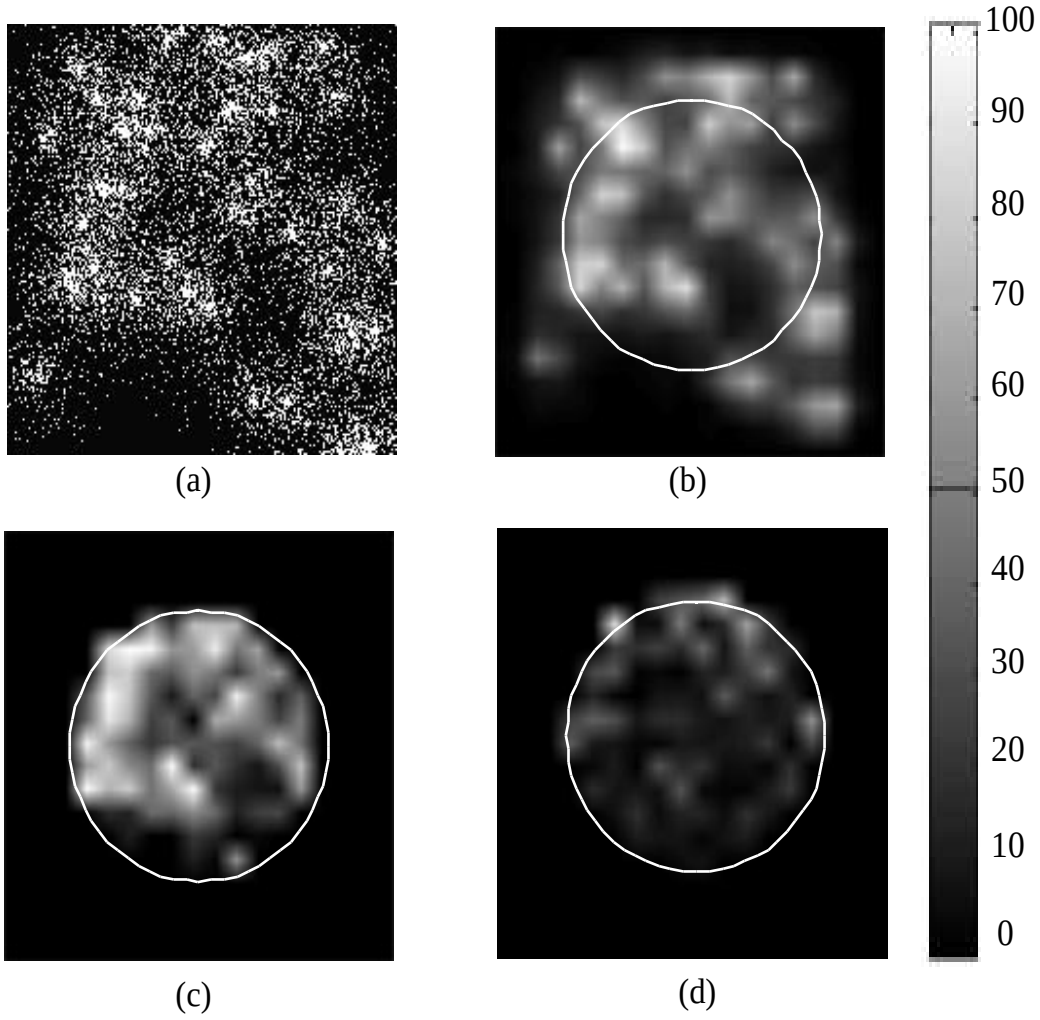

Figure 6. Result of a single inversion simulation including all noise models. (a) source distribution; (b) patched data used for evaluation; (c) reconstructed energy distribution, valid inside the inversion area surrounded by the white circle; (d) absolute error level inside the inversion area. The SNE level is 14.3%. All images are displayed in linear units normalized to the range 0-100.

For the single realisation shown in Figure 6, the reconstructed energy distribution image inside the white circle covers an area of 368 square meters which is split into 100 square patches.

We have observed that the inversion algorithm works robustly if the noise sources and patch resolution size meet the following conditions:

(a) Electronic noise signal-to-noise ratio ≥20 dB,

(b) Beam direction uncertainty ≤ 0.2 degree/step, and

(c) Beam-pattern sensitivity noise consists of ≤ 6 dB reflector imperfection noise and ≤ 2 dB scattered energy noise.

(d) Patch scale ≥2 m.

With combined noise at anticipated levels, the inversion simulation indicates a SNE level ≤ 20% with a patch scale of 2m, providing acceptable source distribution resolution.

5. CONCLUSIONS

This paper presents a stochastic tomographic technique for investigating the temporal and spatial characteristics of shrimp noise in warm shallow water. The novel approach involves several aspects of engineering technologies, such as estimation techniques, computerized tomography, and oceanic acoustics. Through a large number of Monte Carlo simulations, the feasibility of the system has been demonstrated not only under ideal theoretical assumptions but also in realistic situations with various noise models.

With a set of tested parameters, we are able to get a simulated inversion with rms error < 20% within the inversion area, when all noise sources with reasonable levels are considered together. Since the software simulation has been completed with satisfactory results, we have started preparing for the real experiment using geometric parameters found by optimising the error estimates by steepest descent. It appears promising that the spatial and temporal characteristics of snapping shrimp can be revealed on a temporal scale of a few minutes and spatial scales of 2m by the experiment, and the outcome will hopefully contribute to the future explorations of sonar design and applications.

6. REFERENCES

[1] M. J. Buckingham, J. R. Potter and C. L Epifanio. 1997, "Seeing underwater with background noise", *Scientific American.*, February, pp 86-90

[2] D. H. Cato and M. J. Bell, 1991, "Ultrasonic ambient noise in Australian shallow water at frequencies up to 200kHz", *DSTO report MRL-TR-91-23*.

[3] J. R. Potter, F. N. Wu and H. Li, 1997, "A planned tomographic inversion experiment for snapping shrimp; temporal and spatial statistics of these primary noise producers". *Invited paper. The Proceeding of Shallow Water Acoustics Conference*, Beijing April 21-25 1997.

[4] P. H. Pidsley and G. L. Davies, 1995, "Reconstruction of sonar images using computerized tomography", *GEC Journal of Research*, Vol 12(3), pp. 174-180.

[5] E. J. Fremouw and J. A. Secan, 1992, " Application of stochastic inverse theory to ionospheric tomography", *Radio Sci.*, Vol. 27(5), pp. 721-732.

[6] C. L. Lawson and R. J. Hanson, 1974, "Solving least squares problems", *Prentice-Hall Series in automatic computation.*

[7] W. L. Au and K. Banks, 1998, "The acoustics of the snapping shrimp Synalpheus parneomeris in Kaneohe Bay", *J.A.S.A.* Vol. 103(1), pp. 41-47.

[8] W. L. Au and K. Banks, 1996, "The Acoustics of Snapping Shrimp in Kaneohe Bay" (Abstract), *J.A.S.A.* Vol. 99(4), Pt2, pp. 2533.

[9] F. A. Everest, R. A. Young and M. W. Johnson, 1948, "Acoustic characteristics of noise produced by snapping shrimp", *J.A.S.A.*, Vol. 20, pp 137-142.